Environ Ecol Stat (2017) 24:131–150
DOI 10.1007/s10651-016-0363-x

Statistical treatment for the wet bias in tree-ring chronologies: a case study from the Interior West, USA

Yan Sun[1] · **Matthew F. Bekker**[2] · **R. Justin DeRose**[3] · **Roger Kjelgren**[4] · **S.-Y. Simon Wang**[4]

Received: 23 February 2016 / Revised: 17 November 2016 / Published online: 9 December 2016

Abstract Dendroclimatic research has long assumed a linear relationship between tree-ring increment and climate variables. However, ring width frequently underestimates extremely wet years, a phenomenon we refer to as 'wet bias'. In this paper, we present statistical evidence for wet bias that is obscured by the assumption of linearity. To improve tree-ring-climate modeling, we take into account wet bias by introducing two modified linear regression models: a linear spline regression (LSR) and a likelihood-based wet bias adjusted linear regression (WBALR), in comparison with a quadratic regression (QR) model. Using gridded precipitation data and tree-ring indices of multiple species from various sites in Utah, both LSR and WBALR show a significant improvement over the linear regression model and out-perform QR in terms of in-sample R^2 and out-of-sample MSE. This further shows that the wet bias emerges from nonlinearity of tree-ring chronologies in reconstructing precipitation. The pattern and extent of wet bias varies by species, by site, and by precipitation regime, making it difficult to generalize the mechanisms behind its cause. However, it is likely that dis-coupling between precipitation amounts (e.g., percent received as

Handling Editor: Pierre Dutilleul.

✉ Yan Sun
yan.sun@usu.edu

1 Department of Mathematics and Statistics, Utah State University, 3900 Old Main Hill, Logan, UT 84322, USA

2 Department of Geography, Brigham Young University, 690 SWKT, Provo, UT 84602, USA

3 Forest Inventory and Analysis, Rocky Mountain Research Station, 507 25th Street, Ogden, UT 84401, USA

4 Department of Plants, Soils, and Climate, Utah State University, 4820 Old Main Hill, Logan, UT 84322, USA

rain/snow or percent infiltrating the soil) and its availability to trees (e.g., root zone dynamics), is the primary mechanism driving wet bias.

Keywords Dendrochronology · Dendroclimatology · Likelihood-based modeling · Saturation

1 Introduction

Tree-ring-based reconstructions, which provide a means to understanding long-term climate variability, are largely based on the assumption of a linear relationship between year-to-year variation in indices of tree-ring width and climate variables. Although this linearity is the foundation for analyzing the relationship between climate and tree physiological processes, nonlinearities can occur when a limiting environmental factor becomes no longer limiting (Cook and Pederson 2011). For example, in dry regions where low precipitation limits growth ring increment, ring widths often inadequately represent the wettest years; this nonlinearity can lead to reconstructed values that under represent actual values, i.e., the 'wet bias' (Fig. 1). Virtually all stream flow reconstructions based on the tree-ring record have exhibited this bias (Meko and Woodhouse 2011). While a large body of dendroclimatic research seeks to determine the strength, temporal stability, and source of climate-regulated growth increment, much less attention has been paid to the wet bias phenomenon associated with larger ring widths.

The observation that ring width does not strictly scale with high precipitation years is not new. Lundegardh (1931) proposed the Law of Relative Effects as follows (cited in Fritts 1976, p 119):

> The more nearly a factor is in minimum in relation to the other factors acting upon the plant, the greater is the relative influence of a change of that factor upon the growth of the plant. *As a factor increases in intensity, its relative effect upon the plant decreases; and when the factor is in the region of its maximum, the effect of a change upon the plant is nil*

Fritts (1976) further explained the implication of this law for dendrochronology: narrower rings provide more precise climatic information than do wider rings. In other words, when a typically limiting factor becomes abundant, other factors become limiting to varying degrees from one tree to the next, and thus growth patterns among trees can differ considerably.

The most commonly proposed physiological mechanism behind the wet bias invokes the idea that putative carbon acquisition is 'saturated' such that above some threshold, ring-width increment is no longer sensitive to available precipitation (Fritts 1976; Cook and Pederson 2011). Saturation in precipitation (or some other variable) makes intuitive sense in explaining the possible cause behind the wet bias. However, saturation might also be influenced by individual species water-use behavior (e.g., isohydric versus anisohydric) (Meinzer et al. 2014; Bowker et al. 2012). That is, if species maintain stomatal conductance in proportion to evaporative demand we might expect a linear response of ring width to precipitation (isohydric). In contrast, if species regulated stomata along a continuum of soil water demand (anisohydric), carbon allocation might not be proportional, such that wet bias is mostly an issue of timing, i.e., too much water at one time for too small of root zone volume. Recent literature has recognized potential, species-specific trade-offs between leaf-level photosynthetic regulation (i.e., stomatal conductance) and photosynthesis, (e.g., growth and carbon accumulation) (Limousin et al. 2013; McDowell et al. 2008). As a result, the threshold invoked in the 'saturation' hypothesis suggests that the ring width-climate relationship may not be strictly linear across the range of precipitation.

Extreme precipitation events, which likely interact with water use behavior, provide another possible mechanism behind non-linear growth patterns (i.e., wet bias). Common in semi-arid climates, these events may contribute to the yearly precipitation total but the additional water is unavailable to the tree due to run off or percolation below the root zone, and therefore of no benefit to growth. The impact of precipitation that strays outside the root zone may be exacerbated by the standard site selection criteria for dendroclimatology: steep, rocky sites with little soil development will certainly contain trees sensitive to dry years, but during high-precipitation events or wet years only a fraction of the water will enter and linger in the root zone (Fritts 1976). Regardless of the cause, wet bias clearly occurs in dendroclimatology, weakening model fits, and a further understanding of the relationship between, e.g., precipitation and ring width will help us better understand climate conditions and variability.

While there have been previous attempts to statistically scale the variance of dendroclimatic reconstructions to match the dependent data (e.g., McCarroll et al. 2015), lacking in the literature are studies of the relationship between ring width and its putative controlling variable, i.e., precipitation, where statistical tools can be used to determine if empirical dosage thresholds can be obtained and improve model fit. To our knowledge, a modified linear approach to estimate thresholds associated with a wet bias has not been attempted. Using a linear approach can be more parsimonious than complex nonlinear models and inherits interpretability from commonly used linear regressions. In this paper, we explore using a modified linear approach to identify a wet bias threshold in the relationship between tree-ring index and precipitation across a range of four sites and six species (Fig. 1, inset map). Using an empirically driven statistical approach, we hypothesized that the largest tree-ring index values would not be proportional to that year's driving precipitation value, and that this relationship would vary by species (i.e., based on their water use strategy), and total water year precipitation (i.e., dryness).

2 Materials and methods

2.1 Study area and chronology building

As per the 'site selection' and 'species selection' dendrochronology principles, to maximize species response to precipitation we selected populations of precipitation-sensitive species growing near their lower elevational limits on generally south and west-facing slopes (Fritts 1976; Speer 2010; Table 1; Fig. 1 inset map). At each site two increment cores were collected from a minimum of 20 live trees. Increment cores were returned to the lab, dried, mounted and sanded to accentuate the transverse section. Site- and species-specific chronologies were developed using the marker-year approach and list method (Yamaguchi 1991; Speer 2010). Ring-widths were measured using a sliding-stage connected to a microscope and Measure J2X software. Ring-width measurements were verified with program COFECHA using a 50-year window, overlapped by 25 years (Holmes 1983; Grissino-Mayer 2001). COFECHA output was used to infer chronology strength (interseries correlation coefficient). Statistical strength of the chronologies was verified using a leave-one-out approach to calculate the expressed population signal using the dplR package in R, which compares subpopulation signal to that of the hypothetical population (Wigley et al. 1984). Site- and species-specific chronologies were developed in dplR by detrending individual tree-ring series using a cubic smoothing spline with a 50% frequency cut-off at 67% of the series length (Cook and Peters 1981). Series were then averaged using Tukey's biweight robust mean (Cook and Kairiukstis 1990) and prewhitened using autoregressive modeling to create 'residual' chronologies. Chronologies were truncated to a common period from 1900 to 2010 for analysis.

2.2 Climate data

Monthly precipitation and maximum temperature data for each site were extracted from the Parameter-elevation Regressions on Independent Slopes Model (PRISM) to construct site-specific climographs and explore climatic control on ring width (http://www.prism.oregonstate.edu/, Fig. 1). While the argument could be made that station data are purest, there is no such thing as perfect station data, as they all include issues such as missing data, modeled data, etc. We argue that the use of PRISM data extracted site-by-site is likely to be most representative of the actual precipitation that fell on that site as a result of combining multiple observations (stations) with elevation-based (orographic control on precipitation) interpolation of precipitation variability. Surface air temperature and sea surface temperature (SST) data were obtained from the gridded, monthly NOAA Merged Land-Ocean Surface Temperature Analysis (MLOST) V3.5.4 provided by the NOAA PSD Web site at http://www.esrl.noaa.gov/psd/ (Smith et al. 2008). Gridded soil moisture data were derived from the NOAA Climate Prediction Center (CPC) model-calculated monthly soil moisture water height equivalents (hereafter soil moisture) at 0.5° grid spacing (http://www.esrl.noaa.gov/psd/data/gridded/data.cpcsoil.html).

2.3 Ring width response functions

We conducted bootstrapped correlation function analysis between summed 12-month precipitation data and tree-ring chronologies from June of the previous growing season through August of the current growing season using the treeclim package in the R computing environment (Biondi and Waikul 2004; Zang and Biondi 2015). The 12-month 'water-year' period with the highest correlation to each tree-ring chronology was chosen as the independent variable for the statistical analyses (Table 1).

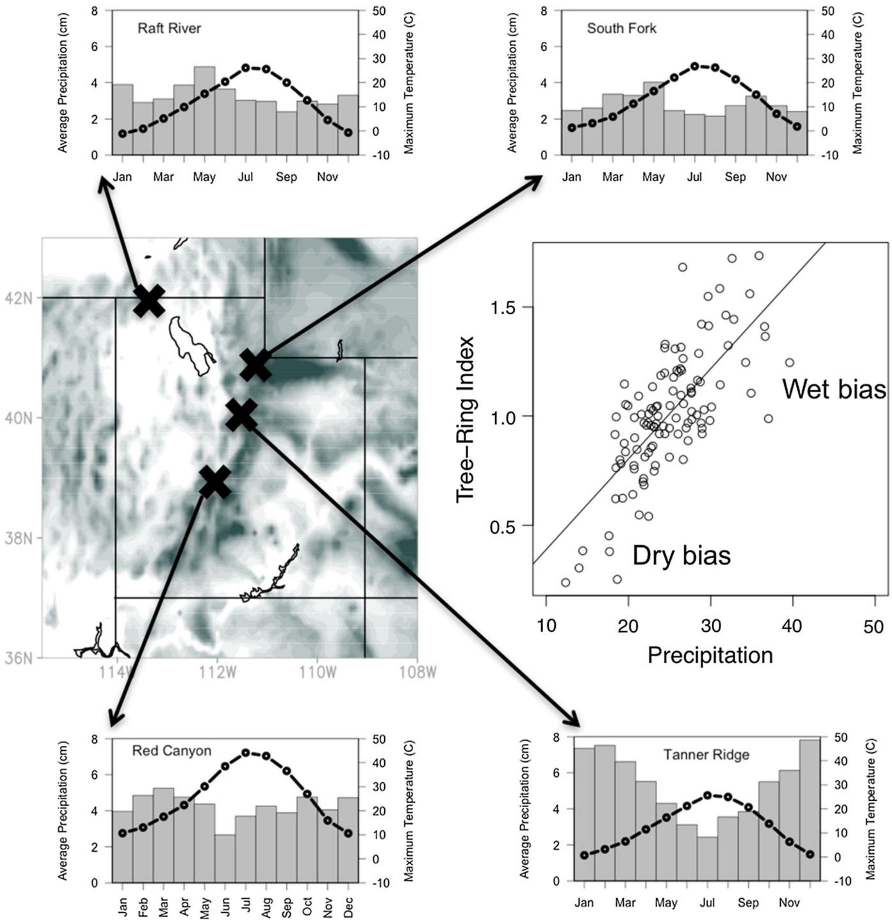

Fig. 1 Study site locations (marked with black **X**), their associated climographs, and scatter diagram between precipitation and the tree-ring index for the Tanner Ridge site (as an example, TRC, TRU in Table 1). Wet biases are marked as those years where tree-ring index values under-predict the precipitation based on LR

2.4 Statistical approach

Biological models of tree growth (i.e., Vaganov-Shashkin) implicitly assume that ring-width is a nonlinear combination of growing season attributes such as temperature and precipitation (Vaganov et al. 1999) and have been effectively used to predict ring width (Anchukaitis et al. 2006). Perhaps the most commonly attempted nonlinear statistical approach to tree-ring reconstruction are artificial neural networks (Woodhouse 1999; QiBin et al. 2000; D'Odorico et al. 2000), which appear to capture both extreme precipitation and overall variability better than linear models (Ni et al. 2002). Other, less common approaches include using response surfaces (Graumlich 1993). To detect wet bias between tree-ring chronologies (not individual series) and yearly precipitation in our study, we first employ linear least squares regression, the most common approach

Table 1 Attributes of the tree-ring chronologies and the precipitation data

Site	Species	Elevation (m)	Latitude (northing)	Longitude (easting)	Interseries correlation	Precipitation (cm)[b]			
						EPS[a]	Min.	Mean (Site)	Max.
Raft river site									
RRS	Singleleaf pinyon	1828	41.95	−113.32	0.774	0.964	18.5	39.8	64.0[c]
Tanner ridge site									
TRC	Common pinyon	1960	40.14	−111.33	0.773	0.955	31.8	50.8	75.2[d]
TRU	Utah juniper	1960	40.14	−111.33	0.711	0.973	31.8		75.2[d]
South fork site									
SFU	Utah juniper	2160	40.92	−111.20	0.810	0.973	16.0	33.6	53.6[d]
Red canyon site									
RCD	Douglas-fir	2280	38.94	−112.06	0.821	0.915	22.9	51.2	80.7[e]
RCB	Bristlecone pine	2280	38.94	−112.06	0.688	0.875	22.9		80.7[e]
RCP	Ponderosa pine	2280	38.94	−112.06	0.699	0.878	29.7		84.3[f]

[a] EPS for the 1900–2010 period. [b] 12-month water-year precipitation from PRISM. [c] 12-month water-year precipitation ending in July. [d] 12-month water-year precipitation ending in June. [e] 12-month water-year precipitation ending in May. [f] 12-month water-year precipitation ending in August

in the study of tree-ring chronologies (Cook and Kairiukstis 1990), and then use that as a baseline for comparison with two novel approaches, linear spline regression, linear maximum likelihood regression, and finally we compute a quadratic regression for comparison purposes.

Throughout the section, we denote by X and Y the precipitation variable and the tree-ring chronology, respectively. The corresponding observations are denoted by $\{x_i, y_i : i = 1, \ldots, n\}$ with n being the sample size. We aim at building regression models that predict Y by X and comparing their empirical performances. Although the ultimate goal of dendroclimatology is to use tree-ring chronologies to infer climate conditions, we chose the other way of modeling because it is more sensible physiologically. In addition, it is of equal importance to thoroughly understand the mechanism behind the growth of a tree ring and how it responds to precipitation, for which the most straightforward and effective strategy is to develop predictive models for Y based on X.

2.4.1 Linear regression (LR)

LR is one of the most common statistical inference models. The model equation of LR is given as

$$Y = aX + b + \varepsilon.$$

Here a, b are fixed regression coefficients, and ε is a mean zero (usually assumed to be normally distributed) random variable with a positive variance σ^2. The coefficients a, b are estimated by the least squares method, which minimizes the sum of squared differences between the observed responses and their linear predictors.

2.4.2 Linear spline regression (LSR)

A linear spline is a continuous function that is piecewise linear. It can be intuitively understood as connected line segments. To account for the wet bias that is possibly contained in the data, we consider the linear spline with one node. Specifically, its model equation is given as

$$Y = a_1 X + a_2 max\,\{X - \theta, 0\} + b + \varepsilon.$$

Here, the constant θ represents a threshold value for X beyond which the wet bias is present. For dry to moderately wet years when X is below θ, the maximum of $X - \theta$ and 0 is 0, and the model equation reduces to LR

$$Y = a_1 X + b + \varepsilon.$$

For the extremely wet years when X is beyond θ, the model equation is seen to be

$$Y = (a_1 + a_2)\, X + (b - a_2\theta) + \varepsilon.$$

The difference between these two equations lies in a_2, which is expected to be negative in view of the wet bias effect. The bigger $|a_2|$ is, the more significant the effect. Especially, when $a_2 = 0$, the two equations coincide with each other and there is no difference between the extreme and non-extreme years. Therefore, the significance t-test for the coefficient a_2 can be used to detect the wet bias.

The model is typically fitted by the least squares method. When fitting the model to the data, θ can be treated either as a preset constant or an additional model parameter to be estimated. In the first scenario, the value of θ can be decided based on physiology (see precipitation cutoffs in Fig. 1). In the second, the value of θ is estimated from statistical optimization scheme that best fits the data. Both cases will be considered in our comparisons.

2.4.3 Wet bias adjusted linear regression (WBALR)

We devise a wet bias adjusted linear regression (WBALR) model that accounts for wet bias using the maximum likelihood (ML) technique. It basically assumes the same model equation as LR, but its parameters are estimated by the ML method, as opposed to the least squares method. The maximum likelihood estimator (MLE) generally requires more effort to compute, but it is statistically more efficient than its least squares counterpart, i.e., MLE has a smaller variance. Especially, the flexibility of likelihood makes it convenient to tackle non-standard cases such as ours.

The key to adjust the linear regression model for wet bias lies in the construction of likelihood function. If there is no wet bias, assuming normal errors, the likelihood for the data $\{x_i, y_i : i = 1, \ldots, n\}$ is defined as

$$
\begin{aligned}
L\left(a, b, \sigma^2\right) &= \prod_{i=1}^{n} l\left(X = x_i, Y = y_i | a, b, \sigma^2\right) = \prod_{i=1}^{n} l\left(\varepsilon = y_i - ax_i - b | a, b, \sigma^2\right) \\
&= \prod_{i=1}^{n} f_\varepsilon(y_i - ax_i - b | a, b, \sigma^2) = \prod_{i=1}^{n} \frac{1}{\sigma\sqrt{2\pi}} e^{-\frac{(y_i - ax_i - b)^2}{2\sigma^2}} \\
&\propto \sigma^{-n} \prod_{i=1}^{n} e^{-\frac{(y_i - ax_i - b)^2}{2\sigma^2}}.
\end{aligned}
$$

Namely, it is the product of the conditional probability density functions of y_i given x_i, $i = 1, \ldots, n$. In the presence of wet bias, Y tends to be overestimated for $X \geq \theta$. This can equivalently be interpreted as that the underlying value of X as the linear predictor for Y is smaller than its observed value. To capture the wet bias while still keeping the simplicity of a linear relationship, we introduce a new variable Z that represents the linear precipitation predictor for Y in replacement of X. Namely, for the entire range of data, we assume the linear equation

$$Y = aZ + b + \varepsilon.$$

Obviously, for $X < \theta$, we can define $Z = X$. When $X \geq \theta$, we do not know the exact value of Z, so we assume that $\theta \leq Z \leq X$. Correspondingly, the likelihood is modified to be

$$L\left(a,b,\sigma^2\right)=\left[\sum_{x_i<\theta}\frac{1}{\sigma\sqrt{2\pi}}e^{-\frac{(y_i-ax_i-b)^2}{2\sigma^2}}\right]*L_1\left(a,b,\sigma^2\right),$$

where $L_1\left(a,b,\sigma^2\right)$ is the likelihood function for the subset $\{x_i, y_i : x_i \geq \theta\}$ computed as

$$L_1\left(a,b,\sigma^2\right)=\prod_{x_i\geq\theta} l\left(\theta\leq Z\leq x_i, Y=y_i|a,b,\sigma^2\right).$$

Define

$$\begin{aligned}\alpha_i &= min\{y_i-a\theta-b, y_i-ax_i-b\},\\ \beta_i &= max\{y_i-a\theta-b, y_i-ax_i-b\}.\end{aligned}$$

Assuming a normal distribution for ε and by using the relationship $Y=aZ+b+\varepsilon$, we have

$$\begin{aligned}L_1\left(a,b,\sigma^2\right)&=\prod_{x_i\geq\theta}P\left(\alpha_i\leq\varepsilon\leq\beta_i|a,b,\sigma^2\right)=\prod_{x_i\geq\theta}\int_{\alpha_i}^{\beta_i}f_\varepsilon(z|a,b,\sigma^2)dz\\ &=\prod_{x_i\geq\theta}\int_{\alpha_i}^{\beta_i}\frac{1}{\sigma\sqrt{2\pi}}e^{-\frac{z^2}{2\sigma^2}}dz=\prod_{x_i\geq\theta}\int_{\theta}^{x_i}\frac{|a|}{\sigma\sqrt{2\pi}}e^{-\frac{(y_i-ax-b)^2}{2\sigma^2}}dx.\end{aligned}$$

Therefore, the complete likelihood function is

$$\begin{aligned}L\left(a,b,\sigma^2\right)&=\left[\prod_{x_i<\theta}\frac{1}{\sigma\sqrt{2\pi}}e^{-\frac{(y_i-ax_i-b)^2}{2\sigma^2}}\right]*\left[\prod_{x_i\geq\theta}\int_{\theta}^{x_i}\frac{|a|}{\sigma\sqrt{2\pi}}e^{-\frac{(y_i-ax-b)^2}{2\sigma^2}}dx\right]\\ &\propto\sigma^{-n}\left[\prod_{x_i<\theta}e^{-\frac{(y_i-ax_i-b)^2}{2\sigma^2}}\right]*\left[\prod_{x_i\geq\theta}\int_{\theta}^{x_i}|a|\,e^{-\frac{(y_i-ax-b)^2}{2\sigma^2}}dx\right].\end{aligned}$$

Then, a, b, σ^2 are estimated by maximizing $L\left(a,b,\sigma^2\right)$. As for prediction, when $x_i < \theta$, y_i is predicted usually as

$$\hat{y}_i=E\left(Y|Z=x_i\right)=ax_i+b.$$

When $x_i\geq\theta$, the predicted value of y_i is calculated by

$$\begin{aligned}\hat{y}_i&=E\left(Y|\theta\leq Z\leq x_i\right)=aE\left(Z|\theta\leq Z\leq x_i\right)+b\\ &=a\frac{EZI_{(\theta\leq Z\leq x_i)}}{P\left(\theta\leq Z\leq x_i\right)}+b=a\frac{\int_\theta^{x_i}zf_Z\left(z\right)dz}{\int_\theta^{x_i}f_Z\left(z\right)dz}+b.\end{aligned}$$

Here $f_Z(\cdot)$ is conveniently assumed to be normal with mean and variance parameters estimated from the data by the maximum likelihood method. In this study, we have assumed a normal distribution for ε. The feasibility of such an assumption can be checked in various ways, i.e., the Kolmogorov–Smirnov test for normality. Generally, other distributions such as Gamma or Student's t can be easily implemented if skewness or heavy-tail is present. Similar to LSR, θ here can be viewed as either a constant or a free parameter; we will consider both cases in our comparisons.

2.4.4 Quadratic regression (QR)

The QR fits a second-degree polynomial to the data. Its model equation is given by

$$Y = a_1 X + a_2 X^2 + b + \varepsilon,$$

and the parameters are estimated by the least squares method. The QR model is the simplest yet very commonly used polynomial model to capture a curved nonlinear pattern. Especially in our case, a quadratic curve could well resemble the shape of wet bias. Although this model falls outside the scope of linear regression and therefore is not comparative to the preceding methods, we included it for comparative purposes to provide further insight into the extent to which the precipitation tree-ring index relationships may be non-linear. If QR fits the tree-ring chronologies better than LSR and WBALR models, it implies that there is a more complicated structure other than the wet bias that lies in the data. Otherwise, if it is competitive or even suboptimal to LSR and WBALR, it is a sign that the wet bias has largely explained the nonlinearity.

2.5 Statistical analysis

First, we fit a linear spline to each of the seven data sets, in the optimal sense that the cutoff point θ is treated as a free parameter to be estimated from data. As we discussed in the previous section, the wet bias corresponds to an upside down V-shaped spline, and the magnitude of this effect can be quantified by the t test for a_2. Next, we compared the in-sample performances of LSR, WBALR, QR, and the baseline model LR. For LSR and WBALR, we considered both preset fixed and data-driven optimal thresholds; the preset values were 90 and 85% quantiles of the precipitation data, respectively. The threshold of WBALR was generally smaller than that of LSR, due to the nature of these two methods. Since these regression models were run on time series data, we checked the residuals for autocorrelation by the Durbin–Watson test. The p values are all well above 0.05, leading to the conclusion of no autocorrelation in the residuals. Additionally, the residuals of WBALR are also checked for normality by the Kolmogorov–Smirnov test and normality is comfortably accepted for all cases. To account for different complexities of these models, we use the adjusted coefficient of determination (R^2) as our comparison criterion, which is defined as

$$Adjusted\ R^2 = 1 - \left(1 - R^2\right) \frac{n-1}{n-p},$$

where n is the sample size, p is the number of parameters in the model, and R^2 is the usual coefficient of determination

$$R^2 = 1 - \sum_{i=1}^{n} \left(y_i - \hat{y}_i\right)^2 / \sum_{i=1}^{n} \left(y_i - \bar{y}\right)^2, \bar{\bar{y}} = \frac{1}{n} \sum_{i=1}^{n} y_i.$$

Namely, the adjusted R^2 assigns heavier penalty to models with more parameters.

Finally, all the methods were evaluated for their out-of-sample performances by randomly splitting each data set into a training set (90%) and a validation set (10%); 100 and 11 data points, respectively. The six models were fitted to the training set, which were then used to compute the mean squared error (MSE) on the validation set, divided by the corresponding sample variances. The process was repeated 100 times independently, and average standardized MSEs for all model/data combinations were calculated (Table 4).

3 Results

We considered seven tree-ring chronologies representing six different species from four different sites (Table 1). The chronologies had series intercorrelations that ranged from 0.69 to 0.82, which indicated very strong climate control on tree-ring width. Precipitation was the primary driver of ring width at all sites with Pearson correlations that ranged from 0.48 to 0.75 (data not shown). Figure 2 shows the fitted linear spline and the linear least squares regression plotted on top of the raw data points. All of the splines consistently show an upside-down V shape, which visually indicates the existence of the wet bias for all data sets. The upside-down V also better fit the associated bias in low precipitation: small ring widths (Fig. 2). The p values of the corresponding significance tests for a_2 are listed in the second column of Table 2.

Statistically significant wet bias was exhibited by Utah juniper (*Juniperus osteosperma*) from two different sites (TRU and SFU), as well as common pinyon (*Pinus edulis*) and ponderosa pine (*Pinus ponderosa*). Bristlecone pine (*Pinus longaeva*) exhibited significant wet bias at the alpha < 0.1 level. Singleleaf pinyon (*Pinus monophylla*) and Douglas-fir (*Pseudotsuga menziesii*) did not pass statistical tests for wet bias. Also listed in Table 2 are the p values for a_2 from the linear spline models where θ is set to be the 90% percentile of the precipitation data. They are generally larger than the optimal p values due to the loss of freedom on θ; however, the statistically significant results match the above mentioned.

In-sample performance between LSR, WBALR, QR, and LR are summarized in Table 3, the value inside the parenthesis in the second-to-last column being the percentile of the optimal threshold for WBALR. We highlight the highest statistic for each data set, which were distributed almost evenly among the three methods of LSR (optimal), WBALR (optimal), and QR. Consistent with Table 2, all the statistics (except for singleleaf pinyon) show moderate to significant improvement over LR. Finally, singleleaf pinyon, which occurred on the second-driest site, exhibited no wet bias, and there was no pattern of improvement above LR.

Based on out-of-sample performance, there was no significant wet bias detected in singleleaf pinyon, so LR had the smallest out-of-sample error (Table 2). For the other sites, models that addressed the wet bias had consistent improvement over LR. Particularly, WBALR worked the best for most of the species. This is because it is

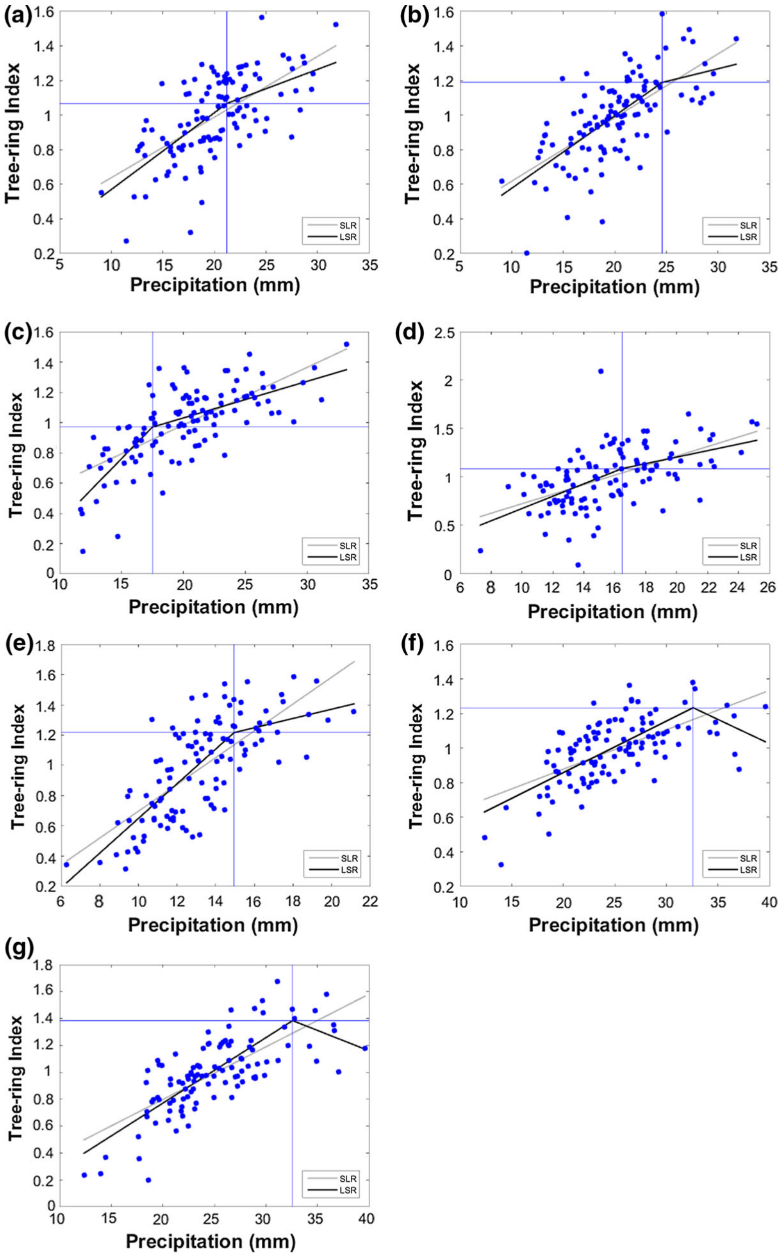

Fig. 2 Fitted LSR using optimal cutoff, compared to the baseline of LR. The *vertical line* denotes the cutoff value for precipitation, and the *horizontal line* denotes the corresponding cutoff value for tree-ring index. *Note* y-axis and x-axis scales differ. The seven plots are: **a** RCB-rcbP5 (precipitation cutoff = 21.21), **b** RCD-rcdP5 (precipitation cutoff = 24.60), **c** RCP-rcpP8 (precipitation cutoff = 17.49), **d** RRS-rrsP7 (precipitation cutoff = 16.47), **e** SFC-sfcP6 (precipitation cutoff = 14.95), **f** TRC-trcP6 (precipitation cutoff = 32.60), and **g** TRU-truP6 (precipitation cutoff = 32.60), respectively

Table 2 Significance test for wet bias

	p value (90%)	p value (optimal)
RCB-rcbP5	0.43105000	0.08146700
RCD-rcdP5	0.14025000	0.12891000
RCP-rcpP8	0.05609500	0.00011578
RRS-rrsP7	0.72854000	0.21298000
SFC-sfcP6	0.00729600	0.00272270
TRC-trcP6	0.00053860	0.00047573
TRU-truP6	0.00023922	0.00020944

The p values are calculated for the t test of coefficient a_2 in LSR. The 2nd column corresponds to the model with θ being the 90% quantile of the precipitation data, and the 3rd column corresponds to θ fitted optimally from the regression

more efficient than the other methods, by making use of the distribution information. Also note QR resulted in better adjusted R^2 (Table 2) but did not necessarily improve MSE (Table 4) for many of the chronologies.

Finally, the comparison between LSR/WBALR and QR is quite interesting and worth noting. On one hand, QR is expected to be a reasonable competitor to LSR/WBALR, since a quadratic curve can well mimic a linear spline. This is reflected in Tables 3 and 4 where QR always produced a statistic very close to the optimal one. On the other hand, given its curvature flexibility, QR did not always give the best fit, indicating that a curved pattern is not really an underlying feature of the data. From the fact that WBALR performed the best for out-of-sample MSE, piecewise linearity is the more precise description of the data. In other words, wet bias may be the key factor contributing to nonlinearity.

4 Discussion

Consistent with our expectations, wet bias is a real phenomenon as determined visually and statistically, but there was no consistent relationship across five species, including four that are commonly used in dendrochronology. The presence of wet bias appeared to be most closely associated with the precipitation regime at a given site, however, it is possible multiple interacting factors ultimately result in the bias. The low-elevation Utah juniper and common pinyon chronologies, both from the same, and highest precipitation, site (Tanner Ridge, Table 1), exhibited significant wet biases, which may suggest precipitation plays a larger role than species (see climographs in Fig. 1). Whereas Douglas-fir and bristlecone pine located on the same site (Red Canyon, Table 1), did not exhibit a statistically significant wet bias, co-occurring ponderosa pine, did show strong wet bias. The species that did not appear to exhibit any wet bias, singleleaf pinyon, occurred on the second-driest site (Raft River, Table 1), and still performed better using LSR, although the model improvement was indistinguishable from LR. In contrast, species that exhibited a wet bias had peak performance that varied between the WBALR and QR. For example, the QR fit best for the co-occurring common pinyon and Utah juniper at Tanner Ridge, but did not necessarily improve MSE. Generally, the WBALR performed the best both in terms of adjusted R^2 and reducing the MSE. The lack of a general relationship for sites or species is conspicuous and requires further analysis.

Table 3 Adjusted R^2 on the complete data

	LR	LSR (90%)	LSR (optimal)	WBALR (85%)	WBALR (optimal)	QR
RCB-rcbP5	0.4136	0.4116	**0.4246**	0.4211	0.4221 (76%)	0.4190
RCD-rcdP5	0.4489	0.4549	0.4556	0.4582	**0.4594 (87%)**	0.4480
RCP-rcpP8	0.4892	0.5017	**0.5510**	0.5080	0.5295 (51%)	0.5330
RRS-rrsP7	0.3034	0.2978	**0.3070**	0.3005	0.3043 (73%)	0.3010
SFC-sfcP6	0.5253	0.5519	0.5593	0.5561	**0.5621 (77%)**	0.5530
TRC-trcP6	0.3831	0.4430	0.4442	0.4305	0.4709 (51%)	**0.4840**
TRU-truP6	0.5259	0.5779	0.5789	0.5721	0.5896 (51%)	**0.5900**

The choice of threshold parameter θ is indicated in the parenthesis next to the model name. The largest value for each species-site combination is highlighted in bold

Table 4 Average standardized MSE on the validation set from 100 independent experiments

	LR	LSR (90%)	LSR (optimal)	WBALR (85%)	WBALR (optimal)	QR
RCB-rcbP5	0.6148	0.6162	0.5977	0.5964	**0.5925**	0.6049
RCD-rcdP5	0.5236	0.5364	0.5187	0.5109	**0.5097**	0.5254
RCP-rcpP8	0.5088	0.5008	**0.4542**	0.4831	0.4663	0.4680
RRS-rrsP7	**0.6431**	0.6508	0.6451	0.6477	0.6446	0.6508
SFC-sfcP6	0.4874	0.4509	0.4418	0.4480	**0.4406**	0.4522
TRC-trcP6	0.6077	0.5481	0.5489	0.5553	0.5137	**0.5068**
TRU-truP6	0.4749	0.4165	0.4146	0.4208	**0.3910**	0.3924

The choice of threshold parameter θ is indicated in the parenthesis next to the model name. The smallest value for each species-site combination is highlighted in bold

4.1 Practical considerations

It has been argued that the small increase in statistical skill as a result of models other than the LR is so trivial as to call into question their use (Hughes 2002). The model improvements documented here are parsimonious (one dependent and one independent variable), ranging between 1 and 9% increase in adjusted R^2 over the LR. In terms of skill, we argue that an improvement up to 9% is notable, considering the relatively limited skill and associated upper limit commonly expected for dendroclimatic reconstructions (i.e., ~70% variance explained). Another important consideration is that our results confirm an expected non-linear relationship between ring width and precipitation. Empirical modeling like that conducted here also corroborates the theoretical expectations of tree growth models (e.g., Vaganov-Shashkin), which presume ring-width increment is a non-linear response of multiple driving factors. Results like this beg for further explanation of the soil-plant-climate mechanistic controls on ring width that create the non-linearity.

Interestingly, while the WBALR and LSR models generally captured the wet bias better, they also appeared to have captured the bias associated with very small ring widths in the lowest precipitation years. This effect is most apparent from the LSR fit for the Utah juniper and common pinyon from Tanner Ridge (Tables 1, 2; Fig. 2). These two chronologies also experienced the largest improvement in skill over LR as a result of WBALR or QR models. Dendroclimatologists commonly select sampling sites that accentuate the low precipitation years, 'marker years' (Fritts 1976), which are incidentally better modeled by the LSR and WBALR approaches. Therefore, the improvement of model fit is likely due to the combined effect of capturing variability in both the high growth years and very low growth years. The combined effect of wet bias years and potentially 'dry bias' years between precipitation and tree-ring indices warrants future scrutiny.

4.2 Wet bias—possible causes

Few studies have determined whether wet bias has a physiological basis given the often-assumed linear nature between tree-ring indices and their climate drivers. A possible explanation is that stressful sites containing long-lived trees are likely sensitive to water stress in part because they grow on coarse-textured and shallow soils. Such soils would have high hydraulic conductance and low water holding capacity, and so excess water from extreme snow or rain events would either run off or percolate below the root zone instead of being retained in a deeper, finer textured soil, exploitable by tree roots. As expected, tree-ring chronologies on water-limited sites trade off pluvial sensitivity for drought sensitivity. Timing of water availability is probably very important to whether the trees can use it or not (growing season versus winter). Regional climate anomalies may also contribute to the formation of wet bias. DeRose et al. (2014) found that the tree-ring reconstruction of Great Salt Lake (GSL) level also featured a prominent wet bias, and exhibited strong low-frequency variability common to the region (Herweijer et al. 2007; Wang et al. 2010, 2012). Because the GSL integrates a broader scale of hydroclimatic anomalies over the region, the

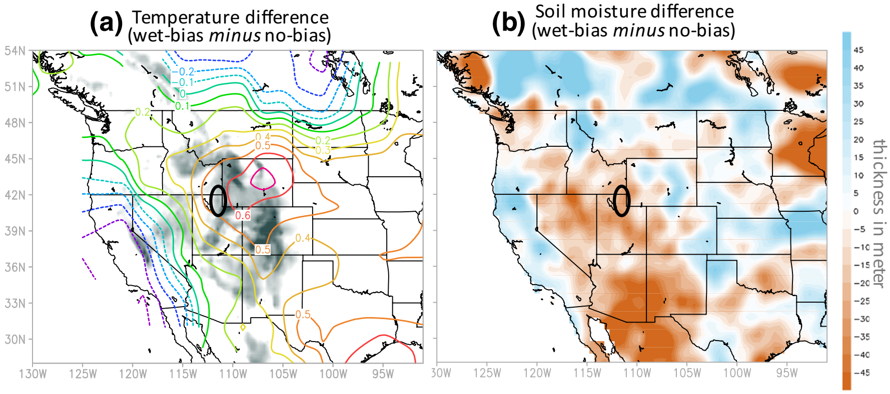

Fig. 3 **a** Surface air temperature anomalies over land between the composites of wet-bias years and "normal" wet years (*contours*), overlaid with topography above 1500 m (*gray shadings*) and a *black circle* indicating approximately the tree-ring sites. **b** Same as (**a**) but for soil moisture anomalies without topography

wet bias revealed from GSL level reconstruction suggests that large-scale climatic conditions indirectly influence tree growth.

To further explore the role of climatic influences on the wet bias, we plotted in Fig. 3a the difference of composite surface temperature between water years of the wet bias group and no bias group identified in Fig. 1. In Fig. 3b we constructed a similar composite difference for soil moisture. It appears that wet-bias years were associated with warmer temperature and associated lower soil moisture. The tree-ring sites (shown in Fig. 3) are located within a region of significantly warmer air temperatures ($p < 0.01$) and marginally significant soil moisture deficit ($p < 0.1$). In those "warmer wet" years (compared to other wet years) the extra precipitation would run off more/faster, rather than being stored as snowpack, before it is made available for the trees to use during the growing season. It could mean that a wet winter followed by a hot summer would lead to over-prediction in ring increment because the excess winter water (which is primarily snowpack in the region) would either sublimate, run off, or percolate below the root zone prior to the growing season, reducing available water for growth. In turn, warmer growing season temperatures would increase evapotranspiration and root zone water depletion. It is possible that any precipitation delivered during the growing season in flashy events, i.e. monsoon-season storms, would mostly percolate below the root zone or run off and only temporarily decrease tree transpiration.

5 Conclusion

Since the publication of Fritts (1976), little research has been conducted to explore the causes and strength of, and correction for, the wet bias phenomenon. Perhaps the wet bias has come to be accepted as a source of error under the common assumption of a linear relationship between tree-ring increment and precipitation (or stream flow)

(Schofield et al. 2016). Our results suggest that wet bias can be addressed causally and statistically. The pattern of wet bias among the studied tree-ring chronologies indicated that species and site (root zone water availability) did not discernably explain wet bias, but a seasonal precipitation effect was discernable. Alternative linear models may be alternative approaches to accounting for wet bias in climate reconstructions. Instead of resorting directly to nonlinear modeling, this paper proposed two modified linear regression models, LSR and WBALR (based on maximum likelihood), which can effectively correct the wet bias while maintaining the parsimony of LR. Compared to nonlinear models, which are usually complicated in nature, the proposed models have the unique advantage of simplicity and interpretability inherited from LR. Specifically, the WBALR was shown to have superior performance by making use of the distribution information, and so is a promising method for improvement in modeling the relationship between tree-ring indices and climate variables.

Acknowledgements The authors would like to thank the editor and two anonymous referees for their valuable comments and suggestions, which have led to a much better presentation of the paper. The Wasatch Dendroclimatology Research Group (WADR) played a crucial role in funding and guiding this project. This research was funded by a U.S. Bureau of Reclamation WaterSmart Grant (No. R13AC80039) and a U.S. Department of Energy Grant (DE-SC0016605). We would like to thank Jennefer Parker on the Logan Ranger District and Billy Preston on the Spanish Fork Ranger District, Uinta-Wasatch-Cache National Forest, Karl Fuelling on the Minidoka Ranger District, Sawtooth National Forest, Del Barnhurst on the Fillmore Ranger District, Fishlake National Forest, and Charley Gilmore for sampling permission. This paper was prepared in part by an employee of the US Forest Service as part of official duties and is therefore in the public domain.

References

Anchukaitis KJ, Evans MN, Kaplan A, Vaganov EA, Hughes MK, Grissino-Mayer HD, Cane MA (2006) Forward modeling of regional scale tree-ring patterns in the southeastern United States and the recent influence of summer drought. Geophys Res Lett. doi:10.1029/2005GL025050

Biondi F, Waikul K (2004) DENDROCLIM2002: a C++ program for statistical calibration of climate signals in tree-ring chronologes. Comput Geosci 30:303–311

Bowker MA, Muñoz A, Martinez T, Lau MK (2012) Rare drought-induced mortality of juniper is enhanced by edaphic stressors and influenced by stand density. J Arid Environ 76:9–16. doi:10.1016/j.jaridenv.2011.08.012

Cook ER, Kairiukstis LA (1990) Methods of dendrochronology: applications in the environmental sciences, vol 394. Kluwer Academic Press, Boston

Cook ER, Pederson N (2011) Uncertainty, emergence, and statistics in dendrochronology. In: Hughes MK, Swetnam TW, Diaz HF (eds) Dendroclimatology: prospects and progress. Developments in paleoenvironmental research, vol 11. Springer, New York, pp 77–112. doi:10.1007/978-1-4020-5725-0

Cook ER, Peters K (1981) The smoothing spline: a new approach to standardizing forest interior tree-ring width series for dendroclimatic studies. Tree-ring Bull 41:45–53

DeRose RJ, Wang S-Y, Buckley BM, Bekker MF (2014) Tree-ring reconstruction of the level of Great Salt Lake, USA. Holocene 24:805–813. doi:10.1177/0959683614530441

D'Odorico P, Revelli R, Ridolfi L (2000) On the use of neural networks for dendroclimatic reconstructions. Geophys Res Lett 27:791–794. doi:10.1029/1999GL011049

Fritts HC (1976) Tree rings and climate, vol 567. Academic Press, New York

Graumlich LJ (1993) A 1000-year record of temperature and precipitation in the Sierra Nevada. Quat Res 39:249–255. doi:10.1006/qres.1993.1029

Grissino-Mayer HD (2001) Evaluating crossdating accuracy: a manual and tutorial for the program COFECHA. Tree Ring Res 57:205–221

Herweijer C, Seager R, Cook ER, Emile-Geay J (2007) North American droughts of the last millennium from a gridded network of tree-ring data. J Clim 20:1353–1376. doi:10.1175/JCLI4042.1

Holmes RL (1983) Computer-assisted quality control in tree-ring dating and measurement. Tree Ring Bull 43:69–78. Cofecha Version 6.06. http://www.ldeo.columbia.edu/tree-ring-laboratory/resources/software
Hughes MK (2002) Dendrochronology in climatology-the state of the art. Dendrochronologia 20:95–116. doi:10.1078/1125-7865-00011
Limousin J-M, Bickford CP, Dickman LT, Pangle RE, Hudson PJ, Boutz AL, Gehres N, Osuna JL, Pockman WT, McDowell NG (2013) Regulation and acclimation of leaf gas exchange in a piñon-juniper woodland exposed to three different precipitation regimes. Plant Cell Environ 36:1812–1825. doi:10.1111/pce.12089
Lundegardh H (1931) Environment and plant development (trans: Ashby E). Edward Arnold, London
McCarroll D, Young GHF, Loader NJ (2015) Measuring the skill of variance-scaled climate reconstructions and a test for the capture of extremes. Holocene 25:618–626
McDowell N, Pockman WT, Allen CD, Breshears DD, Cobb N, Kolb T, Plaut J, Sperry J, West A, Williams DG, Yepez EA (2008) Mechanisms of plant survival and mortality during drought: why do some plants survive while others succumb to drought? New Phytol 178:719–739. doi:10.1111/j.1469-8137.2008.02436.x
Meinzer FC, Woodruff DR, Marias DE, McCulloh KA, Sevanto S (2014) Dynamics of leaf water relations components in co-occurring iso- and anisohydric conifer species. Plant Cell Environ 37:2577–2586. doi:10.1111/pce.12327
Meko DM, Woodhouse CA (2011) Application of streamflow reconstruction to water resources management. In: Hughes MK, Swetnam TW, Diaz HF (eds) Dendroclimatology: prospects and progress. Developments in paleoenvironmental research, vol 11. Springer, New York, pp 231–261. doi:10.1007/978-1-4020-5725-0
Ni F, Cavazos T, Hughes MK, Comrie AC, Funkhouser G (2002) Cool-season precipitation in the southwestern USA since AD 1000: comparison of linear and nonlinear techniques for reconstruction. Int J Climatol 22:1645–1662
QiBin Z, Hebda RJ, QiJun Z, Alfaro RI (2000) Modeling tree-ring growth responses to climatic variables using artificial neural networks. For Sci 46:229–239
Schofield MR, Baker RJ, Gelman A, Cook ER, Briffa KR (2016) A model-based approach to climate reconstruction using tree-ring data. J Am Stat Assoc 111(513):93–106
Smith TM, Reynolds RW, Peterson TC, Lawrimore J (2008) Improvements to NOAA's historical merged land-ocean surface temperature analysis (1880–2006). J Clim 21:2283–2296
Speer JH (2010) Fundamentals of tree-ring research. University of Arizona Press, Tucson
Vaganov EA, Hughes MK, Kirdyanov AV, Schweingruber FH, Silkin PP (1999) Influence of snowfall and melt timing on tree growth in subarctic Eurasia. Nature 400:149–151. doi:10.1038/22087
Wang S-Y, Gillies RR, Jin J, Hipps LE (2010) Coherence between the Great Salt Lake level and the Pacific Quasi-Decadal Oscillation. J Clim 23:2161–2177. doi:10.1175/2009JCLI2979.1
Wang S-Y, Gillies RR, Reichler T (2012) Multidecadal cycles in the Great Basin recorded by the Great Salt Lake: modulation from a transition-phase teleconnection. J Clim 25:1711–1721. doi:10.1175/2011JCLI4225.1
Wigley TML, Briffa KR, Jones PD (1984) On the average value of correlated time series, with applications in dendroclimatology and hydrometeorology. J Appl Meteorol 23:201–213
Woodhouse CA (1999) Artificial neural networks and dendroclimatic reconstructions: an example from the Front Range, Colorado, USA. Holocene 9:521–529. doi:10.1191/095968399667128516
Yamaguchi DK (1991) A simple method for cross-dating increment cores from living trees. Can J For Res 21:414–416
Zang C, Biondi F (2015) treeclim: an R package for the numerical calibration of proxy-climate relationships. Ecography 38(4):431–436

Yan Sun is Assistant Professor of Statistics in the Department of Mathematics and Statistics at Utah State University. Her research interests in statistical methodology include dimension reduction, time series, and set-valued data analysis. Her main areas of interdisciplinary research are climatology and financial econometrics.

Matthew F. Bekker is Associate Professor of Geography at Brigham Young University. His research interests include tree-ring based reconstructions of hydroclimatic variables and ecological disturbances, as well as forest-environment interactions.

R. Justin DeRose is Research Ecologist for the Forest Inventory and Analysis Program, Rocky Mountain Research Station, USDA Forest Service. He is interested in the ecology and dendrochronology of western U.S. forests.

Roger Kjelgren is Professor in the Department of Plants, Soils and Climate at Utah State University. He works in plant physiological responses to the environment, with a particular focus on tree water use and response to water stress.

S.-Y. Simon Wang is Associate Professor of Climate Dynamics in the Department of Plants, Soils and Climate at Utah State University. His research interests include climate diagnostics and prediction, and attribution of extreme events.